Importance of Backscattering Effects in Ballistic Quantum Transport in Mesoscopic Ring Structures

Mincheol Shin, Kyoung Wan Park, Seongjae Lee, and El-Hang Lee

CONTENTS

ABSTRACT

We have found that in the ballistic electron transport in a ring structure, the junction-backscattering contribution is critical for all the major features of the Aharonov-Bohm-type interference patterns. In particular, by considering the backscattering effect, we present new and clear interpretation about the physical origin of the secondary minima in the electrostatic Aharonov-Bohm effect and that of the $h/2e$ oscillations when both the electric and magnetic potentials are present. We have devised a convenient scheme of expanding the conductance by the junction backscattering amplitude, which enables us to determine most important electron paths among infinitely many paths and to gain insight about their contributions to the interference patterns. Based on the scheme, we have identified various interesting interference phenomena in the ballistic ring structure and found that the backscattering effect plays a critical role in all of them.

I. INTRODUCTION

Thanks to the recent progress of the nano-fabrication technology utilizing the semi-conductor hetero-junctions, it has been made possible to study the electron transport properties in a sample whose dimension of interest is well within the coherent length [1]-[5]. In such a system, the ballistic transport, which assumes that the electrons propagate without any deterrence except for the scattering by the sample boundaries and junctions, is thought to be a better description for the electrons' transport. The ballistic electron transport in a ring structure where the Aharonov-Bohm-type interference effects [6] are observable is investigated in this work. A great attention will be paid to the role of the boundary scatterings, especially the backscattering contribution to the interference patterns. Previous theoretical studies on the ballistic transport in the same ring structure [7]-[16] have revealed interesting observations about, among others, the secondary minima in the electrostatic Aharonov-Bohm (A-B) effect [8] and the alternating conductance minima with respect to either the electric potential change or the magnetic potential change when both the magnetic and the electric potential are present in the system [10]. However, the vital role of the junction backscattering on the interference phenomena in the ring structure was not noticed and hence imprecise interpretations about the physical origin of the interferences were given [8]-[10]. One can easily miss the point because it is commonly believed that in the ballistic samples, the backscattering probabilities by the junction should be small enough not to affect the interference patterns much. The role of the backscattering has not been discussed in the normal-metal mesoscopic systems either (or the problem is already too complicated to consider the backscattering alone). We will show in this paper that our results counter to the common belief in that in the *true* ballistic systems the backscattering by the junction in fact contributes critically *even for very small backscattering probabilities*. With the different perspective, we will re-visit the issues of the interference phenomenon characteristic of the system and give new and clear interpretations about their physical origin. These are based on our devising a convenient scheme of expanding the conductance by the junction backscattering amplitude in Section II, which enables us to sort out most important electron paths among infinitely many paths and to gain insight about their contributions to the interference patterns.

II. THEORY

Let us denote s_{ji} as the transmission amplitude from region i to region j of the left junction of Fig. 1, where $i,\ j = 1, 2, 3$. When N, the number of the propagating channels (modes) in the system, is greater than one, s_{ji}'s are N by N matrices with element $(n,\ m)$ denoting the transmission amplitude from mode m of region i to mode n of region j. s_{ji}'s constitute the

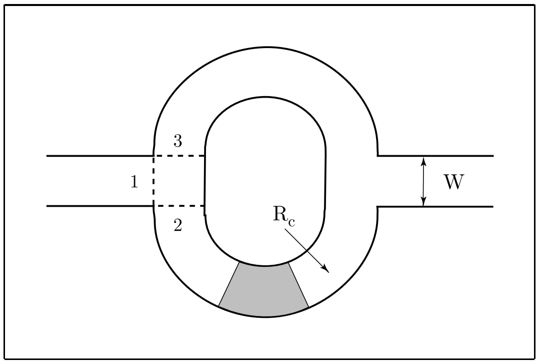

Fig. 1. The ring structure. Shaded is the gate attached on the lower branch of the ring which can modulate the electron's phase θ by the gate electrostatic potential. The regions surrounding the left junctions are indexed. R_C is the central radius of the half ring and w is the width of the wires.

junction S-matrix and satisfy the unitarity condition of $\sum_j |s_{ji}|^2 = 1$ for each i. The transmission amplitude t of the ring structure is given by, assuming the right junction is identical to the left junction,

$$t = (s_{12}Q_1 \; s_{13}P_1)(1-M)^{-1}\begin{pmatrix} s_{31} \\ s_{21} \end{pmatrix}, \qquad (1)$$

where the $2N$ by $2N$ matrix M is defined as

$$M = \begin{pmatrix} s_{33}P_2 & s_{32}Q_2 \\ s_{23}P_2 & s_{22}Q_2 \end{pmatrix} \begin{pmatrix} s_{22}Q_1 & s_{23}P_1 \\ s_{32}Q_1 & s_{33}P_1 \end{pmatrix}, \qquad (2)$$

where P_1 (P_2) is the propagation vector along the lower (upper) branch of the ring in the counterclockwise sense, and Q_1 (Q_2) in the clockwise sense. (1) and (2), which are written for a convenient expansion later in this Section, can be derived from the standard way to express the transmission amplitude t [7]-[10], [17]. When both the magnetic flux threading the ring and the electric potential in either or both of the upper and lower branches are present, we may simply write down the propagators in terms of the magnetostatic Aharonov-Bohm phase shift $\phi \equiv (e/\hbar)\Phi$ where Φ is the magnetic flux threading the ring and the electrostatic Aharonov-Bohm phase shifts θ_1 by the electric potential in the lower branch and θ_2 in the upper branch: the l-th component of the propagation vectors are then

$$\begin{aligned} P_{1,\,l} &= \exp\{i(\phi/2 + \theta_1 + k_l L)\}, \\ P_{2,\,l} &= \exp\{i(\phi/2 + \theta_2 + k_l L)\}, \\ Q_{1,\,l} &= \exp\{i(-\phi/2 + \theta_2 + k_l L)\}, \\ Q_{2,\,l} &= \exp\{i(-\phi/2 + \theta_1 + k_l L)\}, \end{aligned} \qquad (3)$$

where k_l is the wave vector of the electron in the l-th propagating mode and L is the half of the circumference of the ring. For the single propagating channel ($N = 1$), (1) and (2) can be readily solved to give,

$$t = s_{21}^2\{(P_1 + Q_1) - (s_{22} - s_{23})^2 P_1 Q_1 (P_2 + Q_2)\}/D, \qquad (4)$$

where

$$\begin{aligned} D = {} & \{1 - (s_{22}^2 P_2 + s_{23}^2 Q_2)Q_1\}\{1 - (s_{22}^2 Q_2 + s_{23}^2 P_2)P_1\} \\ & - (s_{22}s_{23})^2 P_1 Q_1 (P_2 + Q_2)^2. \end{aligned} \qquad (5)$$

In deriving (4), the exact relationships of $s_{21} = s_{13}$ and $s_{12} = s_{31}$ which can be obtained by the geometrical symmetry and the reciprocity were used. We also set $s_{21} = s_{31}$, $s_{22} = s_{33}$, and $s_{23} = s_{32}$, for simplicity, which is true for zero magnetic field. The dimensionless conductance G for the one-dimensional case is then given by

$$G=|t|^2=4s_{21}^2\{1+\cos\phi\cos\theta-\cos(\chi+2kL+2v)\\ (\cos\phi+\cos\theta)\}/|D|^2, \quad (6)$$

where

$$|D|^2=(1-C_2)^2+4C_1^2-4\cos\chi\{C_1-C_2\cos\chi\\ +C_2C_1\} \quad (7)$$

where

$$C_1=C_1(\phi,\ \theta)\equiv s_{23}^2\cos\phi+s_{22}^2\cos\theta,$$
$$C_2\equiv(s_{22}^2-s_{23}^2)^2,$$
$$\chi\equiv\theta_1+\theta_2,$$
$$\theta\equiv\theta_1-\theta_2,$$

and

$$e^{iv}\equiv s_{22}-s_{23}.$$

(5) gives the exact single-channel conductance at zero temperature.

Once the transmission amplitudes s_{ji} of the junction are known, the conductance can be calculated, either through (6) in the single-channel case or numerically in the multi-channel case via (1) and (2). However, even the analytical expression of (6) does not help us clearly see which paths are responsible for the various interference terms in the equation. Physical origin of the various interesting interference effects of the system, which will discussed in Section III, can not be understood without knowing the paths causing the interferences. We therefore expand (4) by the backscattering amplitude s_{22} (and s_{33}, equally) as follows. To the first order in s_{22} (and s_{33}),

$$t=t_1+t_2+t_3(s_{22},\ s_{33})+O(s_{22}^2)+O(s_{33}^2), \quad (8)$$

where

$$t_1\equiv s_{12}Q_1D_-s_{31},$$
$$t_2\equiv s_{13}P_1D_+s_{21}, \quad (9)$$

and

$$t_3(s_{22},\ s_{33})\equiv s_{12}Q_1D_-(s_{33}P_2s_{23}+s_{32}Q_2s_{33})P_1D_+\\ s_{21}+s_{13}P_1D_+(s_{22}Q_2s_{32}+s_{23}P_2s_{22})Q_1D_-s_{31}, \quad (10)$$

where

$$D_+\equiv(1-s_{23}P_2s_{23}P_1)^{-1},$$
$$D_-\equiv(1-s_{32}Q_2s_{32}Q_1)^{-1}. \quad (11)$$

Then the conductance G approximates

$$G=Tr(tt^+)\approx G_0+G_F+G_B \quad (12)$$

where

$$G_0\equiv Tr(t_1t_1^+)+Tr(t_2t_2^+), \quad (13)$$
$$G_F\equiv Tr(t_1t_2^+)+Tr(t_2t_1^+), \quad (14)$$
$$G_B\equiv Tr((t_1+t_2)t_3^+)+Tr((t_1+t_2)^+t_3)\\ +Tr(t_3t_3^+). \quad (15)$$

In the single-channel case,

$$G_0=1/|D_+|^2+1/|D_-|^2, \quad (16)$$
$$G_F\equiv2\{\cos(\phi+\theta)+s_{23}^4\cos(\phi-\theta)-2s_{23}^2\cos\theta\\ \cos\chi\}/|D_+|^2|D_-|^2, \quad (17)$$
$$G_B=-8s_{22}s_{23}\{s_{23}^2(1+\cos(\phi-\theta))-\cos\chi\\ (\cos\phi+\cos\theta)\}/|D_+|^2|D_-|^2, \quad (18)$$

where

$$|D_+|^2=(1+s_{23}^4-2s_{23}^2\cos(\phi+\chi)), \quad (19)$$
$$|D_-|^2=(1+s_{23}^4-2s_{23}^2\cos(\phi-\chi)). \quad (20)$$

The usefulness of the above expansion may be appreciated by exploring the physical meaning of, or equivalently the paths represented by, the t_i's defined above. First, D_- of (11) can be expanded as follows:

$$D_- = (1 - s_{32}Q_2 s_{32}Q_1)^{-1} = \sum_{n=0}^{\infty}(s_{32}Q_2 s_{32}Q_1)^n. \quad (21)$$

Thus, t_1 can be written as

$$t_1 = s_{12}Q_1 D_- s_{31} = s_{12}Q_1\Big\{1 + (s_{32}Q_2 s_{32}Q_1) + (s_{32}Q_2 s_{32}Q_1)^2 + \cdots\Big\}s_{31}. \quad (22)$$

The first term of (22) represents the electron which initially enters the upper branch of the ring from the left lead, travels along the upper branch clockwise, and at the right junction exits to the right lead. The electron which crosses the right junction and makes one complete turn around the ring clockwise before exiting to the right lead contributes to the second term of (22), and the one which makes two complete turns the third term and so on. Thus t_1 represents the path of the electron circulating in the clockwise sense, with *no* backscattering at the junctions all along its way. Likewise, t_2 is for the electron circulating in the counterclockwise sense without any backscattering. t_3 is the term when there is *only one* backscattering event in the course of the electron's circulation around the ring: the first term of (10) is for the electron which initially rotates counterclockwise, backscatters at a junction, then rotates clockwise untill exiting to the right lead, and the second term the other way around. We can go further to consider more than one backscattering event in the course of the electron's circulation around the ring, which will contribute to the terms of higher order in s_{22}, but in this paper, we will confine ourselves only up to the first order in s_{22} for the following reasons.

That the expansion to the first order in s_{22}, as in (8), could be a sufficiently good approximation for t depends of course on the magnitude of s_{22}, which in turn depends on the so called *coupling* between the ring and the leads [8]-[10]: for the zero coupling, the ring becomes completely isolated from the leads, in which case the backscattering magnitude $|s_{22}|$ should be zero, and on the other hand, for the maximal coupling $|s_{22}|$ should reach its maximum. In the single-channel case, the sole parameter ε in the range between 0 and 1/2 can be designated to control the coupling and one can set $s_{22} = (\sqrt{1-2\varepsilon} - 1)/2$. To the purpose of this paper where the importance of the backscattering will be stressed, we will mainly work within the *very weak coupling* regime in which case the approximation by the expansion only up to the first order in s_{22} is excellent.

Let us digress a little to discuss the coupling between the ring and the leads for the *realistic* systems such as the one in Fig. 1, whose coupling parameter can be obtained by exactly solving the Schröinger equation for the structure [16]-[17]. Fig. 2 shows thus-obtained coupling parameter ε versus the Fermi wave vector k_F for $R_C/w = 5.5$, where the w is the width of the wires and R_C is the central radius of the ring. A single propagating channel is formed in the Fermi wave vector range of (π, 2π), with their boundaries being the transition points to 0 propagating channel and 2 propagating channels, respectively. As one may expect, near the channel boundaries, i.e. near π or 2π, the ring becomes more isolated from the leads, and at the channel center, i.e. near $k_F = 1.5\pi$, the coupling between the ring and the leads are strongest. For the single channel regime, we find that $\varepsilon \leq 0.35$. In the range of the coupling, we can safely approximate the transmission amplitude t by the expansion up to the first order in s_{22}, as in (8). In passing, we note that expansion up to the third order in s_{22} is found to be quite a good approximation for t even for the strongest coupling, i.e. for $\varepsilon = 1/2$ in the single-channel case.

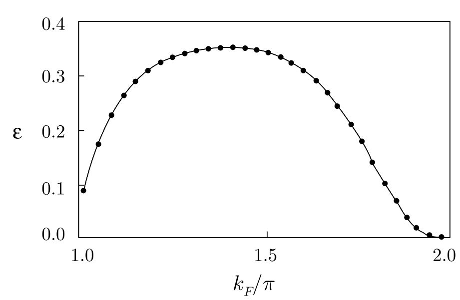

Fig. 2. The coupling parameter ε versus the Fermi wave vector k_F (normalized by π) for the ring structure of Fig. 1 with the central radius $R_C/w = 5.5$.

Although the formalism in this Section holds for any number of propagating channels, we will restrict ourselves to the single-channel transport for the rest of this paper for the sake of simple analysis. The results of (nontrivial) extension to the multi-channel case will be published elsewhere.

III. IMPORTANCE OF THE BACKSCATTERING

We will show in this Section that the backscattering, represented by t_3 of (10) or G_B of (18), plays a crucial role in the ballistic quantum transport in the ring structure, especially in the interference patterns. In the following, the three cases of when there is only the electrostatic potential present, when there is only the magnetostatic potential present, and when both the electrostatic and magnetostatic potential are present are separately discussed.

1. Electrostatic Aharonov-Bohm Effect

We start with simple but intuitive expressions for the t_i's defined in Section II, whereby we drop the resonance terms D_+ and D_- and uninteresting multiplication factors such as s_{12} and s_{31} from them. We can then roughly set

$$t_1 \sim Q_1,$$
$$t_2 \sim P_1, \quad (23)$$

and

$$t_3 \sim P_1 Q_1 (P_2 + Q_2). \quad (24)$$

Note that with these simplified forms, the addition of the three contributions,

$$t_1 + t_2 + t_3 \sim (P_1 + Q_1) + P_1 Q_1 (P_2 + Q_2), \quad (25)$$

already greatly resembles the nominator of the exact t of (4). When only the electrostatic potential is present, the single-channel propagators can be set as

$$P_1 = Q_2 = \exp\{i(\theta + kL)\},$$
$$Q_1 = P_2 = \exp(ikL). \qquad (26)$$

Ignoring the denominators and the multiplication factors, the addition of t_1 and t_2,

$$t_1 + t_2 \sim (P_1 + Q_1) \sim 1 + e^{i\theta} \qquad (27)$$

gives the usual electrostatic A-B interference, and

$$t_3 \sim e^{i(\theta+2kL)}(P_1 + Q_1) \sim e^{i(\theta+2kL)}(1 + e^{i\theta}). \qquad (28)$$

Together,

$$t \sim (1 + e^{i\theta})(1 + e^{i(\theta+2kL)}) \qquad (29)$$

and

$$G \sim (1 + \cos\theta)(1 + \cos(\theta + 2kL)). \qquad (30)$$

The first term in G of (30) gives the usual electrostatic A-B interference, and the second term the so-called "secondary minima" [8]. In Ref. [8], the secondary minima has been attributed to the electron's constructive interference between the one making a full circle around the ring and the one entering the point of entry at the left junction from the left lead. It is obvious, however, from (29) and (30) that the *backscattering* at the junctions represented by t_3 is *necessary* for the occurrence of the secondary minima: that the interference between the two backscattering terms constituting t_3 has the extra phase of $e^{i(\theta+2kL)}$ with respect to the interference between t_1 and t_2 gives rise to the second minima. It is just a *coincidence* that the phase $\theta + 2kL$ in the secondary minima term is identical to the phase gain as the electron makes a full circle around the ring, which may prompt the interpretation such as the one proposed by Cahay *et al*.

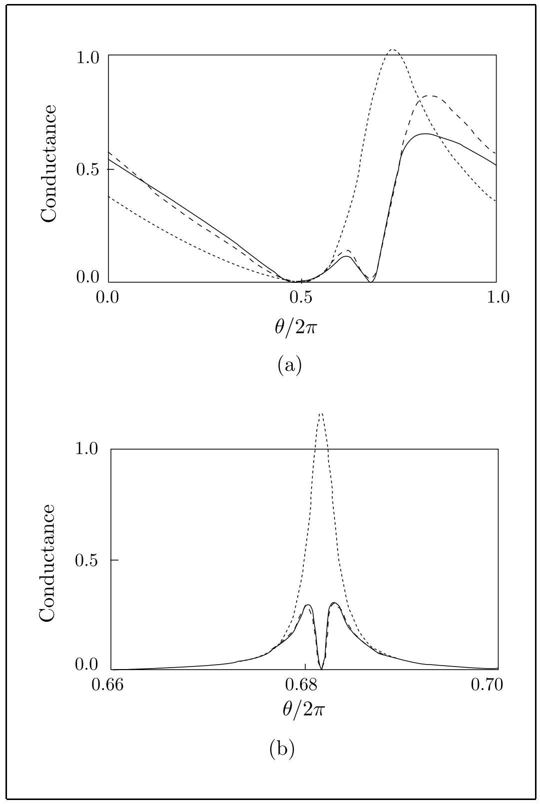

Fig. 3. Various conductances defined in the text versus the electrostatic phase shift θ (normalized by 2π) for $\varepsilon = 0.4$ (a) and 0.01 (b). Solid line is for the full calculation G, dotted line $G_0 + G_F$, and dashed line $G_0 + G_F + G_B$. kL is fixed at 8.25.

To confirm our idea about the origin of the secondary minima, we have evaluated the exact single-channel expressions of G_0, G_F and G_B of (16)-(18) and G of (6) for the coupling parameter ε of 0.4 and 0.01 respectively, and compare in Fig. 3 the full calculation G, the approximation $G_0+G_F+G_B$ and the approximation without the backscattering term G_0+G_F. The approximation to the first order in s_{22} agrees quite well with the full calculation for $\varepsilon=0.4$ and it does excellently for $\varepsilon=0.01$, as is expected for the very small coupling parameter. A clear point in the figure is that *the secondary minimum which is located at $\theta=0.682$ in the figure is not seen without inclusion of the backscattering assisted term of G_B*. Especially, the fact that the sharp secondary minimum develops only if we include the backscattering term G_B, even when the ratio of the backscattering probability and the transmission probability at the junction $|s_{22}|^2/|s_{23}|^2$ is as small as 2×10^{-5} for $\varepsilon=0.01$, supports solidly our claim about the physical origin of the secondary minima. Note that since $|s_{23}|\approx 1$ at the small coupling parameter G_0+G_F include paths of many turns around the ring, which therefore contain the interference proposed by Cahay *et al.* as the responsible mechanism (interference due to the full circulation around the ring) for the secondary minima.

2. Magnetostatic Aharonov-Bohm Effect

When only the magnetic flux is present in the system, we can set,

$$P_1=P_2=\exp\{i(\phi/2+kL)\},$$

$$Q_1=Q_2=\exp\{i(-\phi/2+kL)\}. \quad (31)$$

Then,

$$t_1+t_2\sim P_1+Q_1\sim 1+e^{i\phi} \quad (32)$$

gives the usual magnetostatic A-B interference, and

$$t_3\sim e^{2ikL}(P_1+Q_1)=e^{2ikL}(1+e^{i\phi}). \quad (33)$$

Together,

$$t\sim(1+e^{i\phi})(1+e^{2ikL}) \quad (34)$$

and

$$G=|t|^2\sim(1+\cos\phi)(1+\cos 2kL). \quad (35)$$

We can thus see that t_3 is *in phase* with t_1+t_2 in terms of the magnetic flux change ϕ so it does not produce any extra effect on the usual magnetostatic AB oscillations. Instead, the effect of the backscattering represented by t_3 is to modulate the amplitude of G with respect to the wave vector k.

Returning to the exact treatment for the t_i's, let us focus on the special minima in the conductance in a sweep by the wave vector k while ϕ is fixed: the exact single-channel conductance formula of (6) gives that the conductance vanishes identically when $2kL+v=(2n+1)\pi$, where n is an integer. (Note that the crude expression of (35) also has the feature that G becomes identically zero when $2kL=(2n+1)\pi$.) That G vanishes at the special points is impossible without the backscattering term t_3 and hence G_B is illustrated in Fig. 4. In the figure, we have evaluated the single-channel expressions of G_0+G_F and G_0+G_F+

G_B of (16)-(18) and also the exact expression for G of (6). There the coupling constant ε is taken to be 0.1 at which the ratio of the backscattering and the forward transmission at the junction $|s_{22}|^2/|s_{32}|^2 \cong 3\times 10^{-3}$. The ratio may lead one to believe that the backscattering contribution should be negligible and G should be well approximated by G_0 and G_F only. However, as the figure clearly shows, small the backscattering may be, only when we include its contribution, we get the proper minima in the conductance.

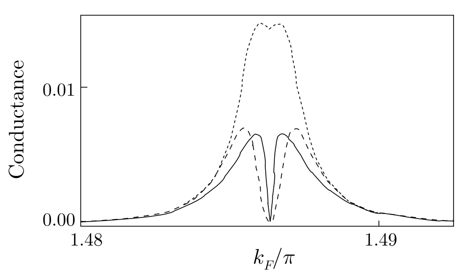

Fig. 4. The same as in Fig. 3 but with respect to k_F (normalized by π). The parameters used are: $L = 5.5\pi$ and $\phi/2\pi = 0.01$.

3. In the Presence of Both the Magnetic and the Electric Potentials

In both the magnetostatic and the electrostatic A-B effects, the interference term of P_2+Q_2 from t_3 was identical to the interference P_1+Q_1 from t_1 and t_2. (See (26) and (31).) Only when the magnetic flux and the electrostatic potential are present simultaneously, they can be distinguished: the simplified expressions for t_i's gives, using the single-channel propagators of (3),

$$t_1+t_2 \sim P_1+Q_1 = 2e^{i(\theta/2+kL)}\cos(\phi/2+\theta/2),$$
$$t_3 \sim P_1 Q_1 (P_2+Q_2) = 2e^{i(\theta/2+kL)} e^{i(\theta+2kL)} \cos(\phi/2-\theta/2). \quad (36)$$

So,

$$t \sim \{\cos(\phi/2+\theta/2) + e^{i(\theta+2kL)}\cos(\phi/2-\theta/2)\} \quad (37)$$

and

$$G \sim (1+\cos\phi\cos\theta) + \cos(\theta+2kL)(\cos\phi+\cos\theta). \quad (38)$$

We can see that the usual forward interference of t_1+t_2 gives the phase shift of $\phi+\theta$ while the backscattering-assisted term of t_3 gives the phase shift of $\phi-\theta$, which is also clearly seen in the expressions of G_F and G_B of (17) and (18).

In the previous discussions of the magnetostatic A-B and electrostatic A-B effects, the role of the denominators of t_i's was not emphasized, although taken into account in the exact treatments, partly because the numerators only could explain major features of the interference patterns (minima) that we were interested in and partly because the fact that the two denominators D_+ and D_- are identical greatly lifts further complications. In the current investigation of the magneto-electrostatic A-B effect, however, we find that the two non-degenerate denominators importantly alter the interference patterns which would have been much simpler with the numerators only, such

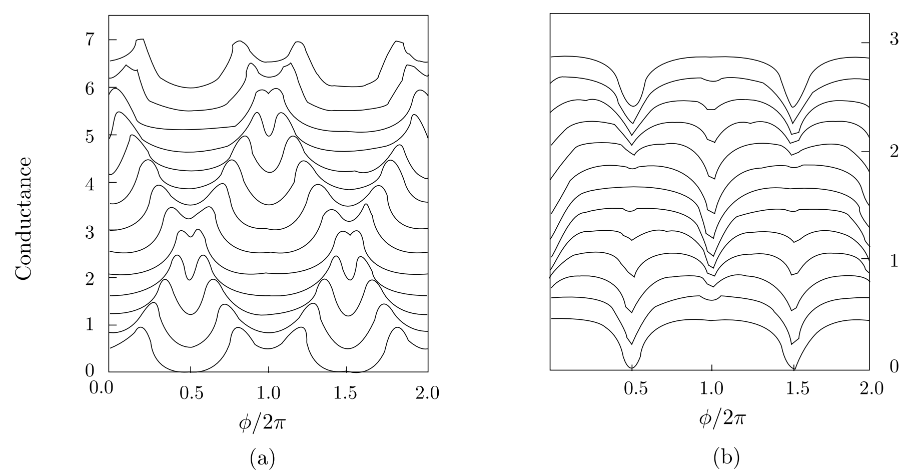

Fig. 5. The conductance G versus the magnetic flux ϕ (normalized by 2π) for different electrostatic phase shifts at zero temperature (a) and at a high temperature (b). The electrostatic phase shift θ is zero for the bottommost curves and increments linearly up to the topmost curves where θ is 2π. kL is fixed at 8.25 for both figures.

as (38). Complications by inclusion of the denominators beat us in any attempt for a simple analysis of the conductance behavior in the form of (6). We have nevertheless found that at zero temperature, the conductance G can be well approximated by

$$G \approx G_0 = 1/|D_+|^2 + 1/|D_-|^2 \qquad (39)$$

if the coupling parameter ε is not too close to 1/2. And at a sufficiently high temperature, G can be derived to be, approximately,

$$G \sim s_{22}(1+\cos\phi\cos\theta)/(1+s_{23}^2\cos 2\phi). \qquad (40)$$

By the sufficiently high temperature we mean the temperature above which the temperature averaging of the conductance, which is

$$G(T) = \int dk_F \left(-\frac{df}{dk_F}\right) G\ (k_F; T=0), \qquad (41)$$

where f is the Fermi distribution, becomes practically independent of the temperature, that is, the cosine terms containing the Fermi wave vector k_F in the zero-temperature conductance become completely averaged out. At $T=0$, the term $\cos(\phi+\theta)$ in $|D_+|^2$ and the term $\cos(\phi-\theta)$ in $|D_-|^2$ of (39) give rise to the two sets of peaks running in the opposite directions in the conductance plot against the magnetic flux ϕ and the electric potential θ. See Fig. 5(a). In the high temperature limit, the two sets of the conductance minima in the plot against ϕ alternate with θ as follows. (See Fig. 5(b).) At $\theta = 0$, only one set of minima located at $\phi = \pi$ and 3π are visible, but as θ increases from 0, the second set of minima located at $\phi = 0$ and 2π develop and become deeper while the minima located at π and

3π become shallower. The development of the second set of the minima and the diminution of the first set of the minima continue until $\theta = \pi$, where only the second set of minima are now visible. In the meanwhile, at $\theta = \pi$ the two sets of the minima become equal in their depth so as to make it appear that the period of the conductance oscillations with respect to ϕ is π. The same process repeats as θ increases further from π, with the role of the first and the second set of minima reversed. Note that this behavior is well accounted for by the concise form of (40).

It is the high temperature limit that the backscattering contribution by G_B is absolutely necessary for the behavior mentioned above. The point is clearly illustrated in Fig. 6 where G (the full calculation without any approximation), G_0, G_F, G_B, and $G_0 + G_F + G_B$ are shown when $\theta = \pi/2$. We first note that the full calculation G is well approximated by the summation, $G_0 + G_F + G_B$, of the three contributions. G_0 is almost constant in this high temperature limit and G_F and G_B look shifted by π from each other. When G_F and G_B are added together, their original 2π oscillations cancel out and produce the π oscillation: this is in effect equivalent to the vanishment of the ϕ dependence term in the numerator of the expression (40) when $\theta = \pi/2$ and only the denominator which has the period of π influence the conductance oscillations. The authors of Ref. [10] only dealt with the zeroes of the numerator of the conductance in (6) to explain the minima of the π oscillations, whereby they did not give any physical origin of the oscillations anyway. It is now clear from our analysis that the zeroes of the numerators just coincided with the minima at $\theta = \pi/2$ and that the multiplications of the two resonance terms, $|D_+|^2$ and $|D_-|^2$, as the result of the addition of the forward-interference contribution and the backscattering contribution, give rise to the desired π oscillations. As in the case of the electrostatic or magnetostatic A-B effect, we again emphasize that one cannot obtain the proper interference patterns without the backscattering contribution, *however small it may seem by looking at the backscattering probability at the junctions*.

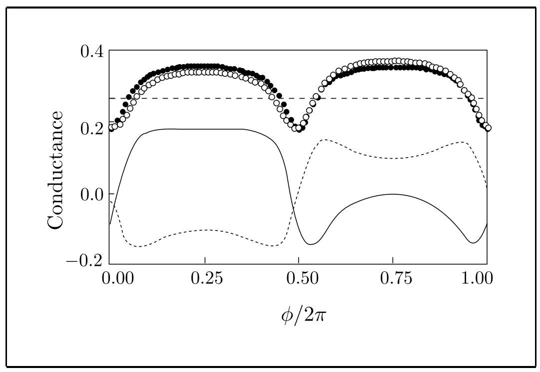

Fig. 6. The various conductances at a high temperature when the magnetic and electric potentials are simultaneously present. θ is fixed at $\pi/2$ and $L = 5.5\pi$. The legends are: solid circles for G, open circles for $G_0 + G_F + G_B$, dashed line for G_0, solid line for G_F, and dotted line for G_B.

IV. CONCLUSION

We have presented that the major features of the Aharnov-Bohm-type oscillations in the ballistic limit cannot be explained without considering the backscattering contribution originated from the electrons' scattering by the junctions. We have expanded the conductance in terms of the backscattering amplitude at the junction and showed that the expansion only up to the first order can be used to successfully account for the backscattering contributions in the various interference phenomena. In particular, the physical origin of the secondary minima in the electrostatic A-B effect and that of the π oscillations in the magneto-electrostatic A-B effect have been clarified by the consideration of the backscattering contribution.

ACKNOWLEDGEMENT

This work has been supported by the Ministry of Information and Communications of Korea.

REFERENCES

[1] R. A. Webb, S. Washburn, C. P. Umbach, and R. B. Laibowitz, "Observation of h/e Aharonov-Bohm oscillations in normal-metal rings," *Phys. Rev. Lett.,* vol. 54, no. 25, pp. 2696-2699, 1985.

[2] G. Timp, A. M. Chang, P. Mankiewich, R. Behringer, J. E. Cunningham, T. Y. Chang, and R. E. Howard, "Quantum transport in an electron-wave guide," *Phys. Rev. Lett.,* vol. 59, no. 6, pp. 732-735, 1987.

[3] B. J. van Wees, H. van Houten, C. W. J. Beenakker, J. G. Williamson, L. P. Kouwenhoven, D. van der Marel, and C. T. Foxon, "Quantized conductance of point contacts in a two-dimensional electron gas," *Phys. Rev. Lett.,* vol. 60, no. 9, pp. 848-850, 1988.

[4] C. J. B. Ford, T. J. Thorton, R. Newbury, M. Pepper, H. Ahmed, C. T. Foxon, J. J. Harris, and C. Roberts, "The Aharonov-Bohm effect in electrostatically defined heterojunction rings," *J. Phys. C: Solid State Phys.,* vol. 21, pp. L325-L331, 1988.

[5] P. G. N. de Vegvar, G. Timp, P. M. Mankiewich, R. Behringer, and J. Cunningham, "Tunable Aharonov-Bohm effect in an electron interferometer," *Phys. Rev. B,* vol. 40, no. 5, pp. 3491-3494, 1989.

[6] Y. Aharonov and D. Bohm, "Significance of electromagnetic potentials in the quantum theory," *Phys. Rev.,* vol. 115, no. 3, pp. 485-491, 1959.

[7] Y. Gefen, Y. Imry, and M. Ya. Azbel, "Quantum oscillations and the Aharonov-Bohm effect for parallel resistors," *Phys. Rev. Lett.,* vol. 52, no. 2, pp. 129-132, 1984.

[8] M. Cahay, S. Bandyopadhyay, and H. L. Grubin, "Two types of conductance minima in electrostatic Aharonov-Bohm conductance oscillations," *Phys. Rev. B,* vol. 39, no. 17, pp. 12989-12992, 1989.

[9] S. Bandyopadhyay and W. Porod, "Double quantum wire Aharonov-Bohm interferometers for possible LN2 temperature operation," *Superlattices and Microstructures,* vol. 5, no. 2, pp. 239-245, 1989.

[10] Daisuke Takai and Kuniichi Ohta, "Aharonov-Bohm effect in the presence of magnetic flux and electrostatic potential," *Phys. Rev. B,* vol. 48, no. 3, pp. 1537-1543, 1993.

[11] Daisuke Takai and Kuniichi Ohta, "Electrostatic Aharonov-Bohm conductance oscillations in a mesoscopic ring: effect of potential discontinuities," *Phys. Rev. B,* vol. 49, no. 3, pp. 1844-1847, 1994.

[12] W.-C. Tan and J. C. Inkson, "Landau quantization and Aharonov-Bohm effect in a two dimensional ring," submitted to Phy. Rev. B, 1995.

[13] S. Datta, "Quantum devices," *Superlattices and Microstructures,* vol. 6, no. 1, pp. 83-93. 1989.

[14] S. Datta and S. Bandyopadhyay, "Aharonov-Bohm effect in semiconductor microstructures," *Phys. Rev. Lett.,* vol. 58, no. 7, pp. 717-720, 1987.

[15] S. Datta and M. R. Melloch, S. Bandyopadhyay, R. Noren, M. Vaziri, M. Miller, and R. Reifenberger, "Novel inerference effects between parallel quantum wells," *Phys. Rev. Lett.,* vol. 55, no. 21, pp. 2344-2347, 1985.

[16] Mincheol Shin, Kyoung Wan Park, Seongjae Lee, and El-Hang Lee, "Quantum interference effects in an Aharonov-Bohm ring with a gate," *Jpn. J. Appl. Phys.,* vol. 34, part 1, no. 8B, pp. 4470-4472, 1995.

[17] Mincheol Shin, Kyoung Wan Park, Seongjae Lee, and El-Hang Lee, "Crossover behavior of the conductance oscillations in a quasi-one dimensional ring in the ballistic limit," Phys. Rev. B, vol. 53, no. 2, pp. 1014-1017, 1996.

Mincheol Shin was born in Hong Sung, Korea in 1965. He received the B.S. degree in physics from Seoul National University, Seoul, Korea in 1988 and the Ph.D. degree in physics from Northwestern University, Evanston, Illinois, USA in 1992. Since 1993, he has been with Research Department in ETRI work-ing on theoretical modellings and calculations for mesoscopic systems.

Kyoung Wan Park was born in Seoul, Korea in 1956. He received B.S. and M.S. degrees in physics from Seoul National University, Seoul, Korea in 1978 and from Korea Advanced Institute of Science, Seoul, Korea in 1981, respectively, and his Ph.D. degree in physics from North Carolina State University, Raleigh, North Carolina, U.S.A., in 1990. From 1981 to 1984, he was a researcher with the Optics Laboratory of Korea Standards Research Institute. In 1990, he joined Research Department in ETRI. His research interests include thin film growth of semiconductors, surface treatments and optical measurements on compound semiconductors, and mesoscopic phenomena.

Seongjae Lee was born in Korea in 1957. He received a B.S. degree from Seoul National University in 1980, M.S. degree from Korea Advanced Institute of Science in Seoul, Korea in 1982, and Ph.D. degree in Physics from Northwestern University in Illinois, U.S.A. in 1991. Currently he is working in Research Department in Electronics and Telecommunications Research Institute in Taejon, Korea. His research interests are in the electrical transport of the metallic and superconducting systems with reduced dimensions, the mesoscopic systems of metal or semiconductor and the device applications of the mesoscopic systems.

El-Hang Lee

See *ETRI Journal*, vol. 17, no. 2, p. 10, July 1995.